Communication

Optimized Transmitting Sources for Radiative Wireless Power Transmission With Lossy Media

Joon-Hong Kim and Sangwook Nam

Abstract—**This communication presents a method for the theoretical analysis of the radiative wireless power transmission (R-WPT) in lossy environments. We identified the efficiency bounds for specific receiver antennas when the available transmission area was limited. In addition, the optimal transmission currents were obtained and used to determine the proper location and polarization of the transmitting array. It was found that the fields emitted from the receiver in the transmitting mode are an important factor for determining the efficiency bound. To understand the R-WPT with lossy media better, the proposed theoretical framework was applied to two examples. The efficiency bounds for the examples were compared with the results obtained using previous works to assess the usability of the proposed theory. This study could serve as a basis for the development of R-WPT systems for practical microwave transmission applications with lossy objects.**

Index Terms—**Fresnel zone, implantable devices, lossy media, microwave power transmission, optimization, phase conjugation (PC), power transfer efficiency (PTE), radiative near-field, time-reversal, wireless power transmission (WPT).**

I. Introduction

Radiative wireless power transmission (R-WPT) has become a topic of interest in recent years, as it can achieve wireless power transmission (WPT) by increasing the operating ranges and spatial usability. Research on microwave power transfer, which transfers energy using propagating electromagnetic (EM) waves, has been on-going since the 1960s [1]–[4]. The studies in [1]–[3] found the optimal transmitting source for ideal receiving apertures in the Fresnel region by solving EM problems. In [4], the optimal transmitting source and maximum efficiency bound were studied for the receiving antennas in practical applications. However, these studies assumed lossless environments and did not consider the cases in which lossy materials and scatterers exist, which represent more practical scenarios.

Nowadays, studies on WPT in lossy media have been actively reported [5]–[15]. The fundamental studies on antennas immersed in dielectric lossy media are presented in [5] and [6]. Shams and Ali [7] and Jiang and Georgakopoulos [8] demonstrated a WPT to sensors embedded in concrete blocks, showing the feasibility of a low-cost and reliable health monitoring system for infrastructure. Poon *et al.* [9] analytically showed that the optimal frequency is above 1 GHz for tissue layers, which indicates WPT in radiative near-field regions. They suggested mid-field power transfer for implantable medical device (IMD) applications. Based on a theoretical analysis presented in [9], the optimal transmission current for a small implanted receiver was studied in [10]. The authors determined the upper limit of the power transfer efficiency (PTE) with respect to the operating frequency. Das and Yoo [11] studied wireless power transfer to an implantable conformal antenna in the radiative near-field region. They added a near-field plate to the transmission antenna, proposed in [11], to mitigate the leakage power and improve the PTE. In [12] and [13], the phase conjugation (PC) method was used to focus the transmitting power to movable implanted receivers. The transmitter and receiver antennas using magnetic current were designed to reduce tissue losses in [12]. In [13], the proposed PC method was compared with the uniform excitation method; the former method gave better field focusing and specific absorption rate (SAR). However, there has been little discussion on determining the maximum efficiency with respect to the size of the transmitter. In addition, it is difficult to give a physical interpretation on the optimal solutions obtained from the previous analysis.

Duan *et al.* [14], Chen *et al.* [15], Geyi [16], and Shan and Geyi [17] report optimal design procedures to efficiently implement R-WPT systems for general environments. The authors provide both theoretical and practical ways to maximize the PTE. Chen *et al.* [15] and Geyi [16] optimized the excitation of transmission array antennas by solving an eigenvalue problem and demonstrated its usability in various scenarios. Shan and Geyi [17] inserted an implanted antenna in a head phantom and studied the optimal PTE in terms of the number of transmitting arrays and the operating distance. On the other hand, in [18] and [19], conformal near-field focusing for relatively large receiving antennas was proposed. Chou [18] proposed that matching the conformal wavefront of the receiving apertures could maximize the reaction factor, while suggesting a virtual focal point for large receiving arrays. However, there was lack of information to determine the optimal location of the transmitting array elements and efficiency bound for nonideal receiving antennas, especially when lossy scattering objects existed. Furthermore, it is practically hard to measure several scenarios that vary the placement, antenna type, and arrangement of transmitting array antennas to find the maximum efficiency and optimal placement of the transmitter.

This communication presents an analytical study on the optimal transmission current that can maximize the PTE in lossy media. This theoretical analysis uses reciprocity and mathematical substitutions to simplify the solving process, and the corresponding solutions can be intuitively understood. Based on our analysis, the fundamental efficiency bound can be determined when the area of the transmission currents is limited. Furthermore, the optimal locations for the transmitting arrays can be obtained. To demonstrate the significance and applicability of the proposed theory, two examples consisting of implantable scenarios and scattered environments are also presented and discussed.

This study is distinctly novel when compared with previous research. First, the proposed theory provides a method to determine the optimal position of the transmitters for R-WPT with lossy media.

Manuscript received November 11, 2020; revised July 13, 2021; accepted September 13, 2021. Date of publication October 14, 2021; date of current version April 7, 2022. This work was supported by the National Research Foundation of Korea (NRF) grant funded by the Korea Government (MSIP) under Grant 2016R1E1A1A01943375. *(Corresponding author: Sangwook Nam.)*

Joon-Hong Kim is with the Samsung Research, Seoul 06765, South Korea (e-mail: jhong7.kim@samsung.com).

Sangwook Nam is with the School of Electrical Engineering and INMC, Seoul National University, Seoul 151-742, South Korea (e-mail: snam@snu.ac.kr).

This article has supplementary material provided by the authors and color versions of one or more figures available at https://doi.org/10.1109/TAP.2021.3118847.

Digital Object Identifier 10.1109/TAP.2021.3118847

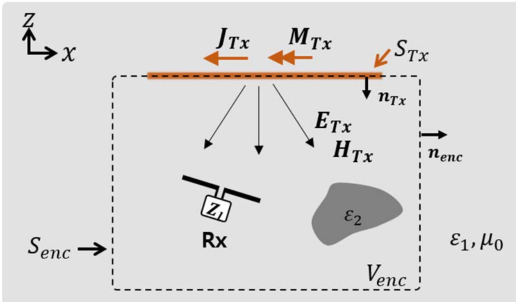

Fig. 1. R-WPT scenario in lossy media. The receiver antenna is buried in the lossy media, and the transmitter is located away from the receiver. This scenario could be extended to general multilayer or scattered environments.

Second, the theory is expressed in simple terms so that its physical meanings are easily revealed. Third, the results not only provide the fundamental efficiency bound but also provide design guidelines to estimate the required transmitter size even in the presence of complex scattering objects.

II. Theory

We first assume a scenario wherein a receiving antenna is buried in lossy media, as shown in Fig. 1. The permeability of the material is set to the value of free space (μ_0), while permittivity values differ. The transmission currents that send wireless power are assumed to be an arbitrary distribution. The transmission surface, where electric current ($\mathbf{J_{Tx}}$) and magnetic current ($\mathbf{M_{Tx}}$) exist, can be formed into any shape such as curved or angled; we assumed a simple planar structure. We define S_{Tx} as the area of the surface where transmitting currents flow. S_{enc} is defined as the entire enclosed surface surrounding the receiver, which includes S_{Tx}. V_{enc} is the volume inside S_{enc}, as shown in Fig. 1.

Notably, we only considered the radiative region where propagating fields are dominant over evanescent fields in the following analysis. The radiative region is defined as that where $kr > 1$, where k is a wavenumber, and r is the distance from a Huygens source. Therefore, the methodology presented in this study cannot be applied to regions where evanescent fields are dominant, such as those very near current sources or scatterers. It is worth mentioning that the radiative region is different from the reactive or radiative near-field regions. For example, let us consider a transmitting array antenna with an electrically large size. The array antenna can be considered as the sum of the equivalent Huygens sources (or point sources). Then, the reactive evanescent fields will exist only near each point source, even if the evanescent fields are added. However, the boundary of the reactive near-field is defined as the phase difference between the emitted fields by each part of the array [20], [21]. This implies that the boundary of the reactive near-field is different from the radiative region that is assumed for the R-WPT. Therefore, this method could be applied from the part of reactive near-field region to the far-field.

A. Problem Formulation

The objective of this study is to identify and then find a method to maximize the efficiency of R-WPT in a lossy medium. The derivations of the formula are described in the supplementary material. The PTE, η, is defined as the ratio of the power received at the load of the receiver antenna (P_{rec_Rx}) to the power emitted by the current on the transmitting surface (P_{in_Tx}), which is the concept of operating gain. Therefore, the PTE can be expressed as

$$\eta = \frac{P_{rec\_Rx}}{P_{in\_Tx}}. \tag{1}$$

First, the transmission power, P_{in_Tx}, can be considered to be the radiating power from the transmission currents. To avoid using the field quantities (i.e., $\mathbf{E_{Tx}}, \mathbf{H_{Tx}}$) emitted by the unknown transmission currents (i.e., $\mathbf{J_{Tx}}, \mathbf{M_{Tx}}$), which require complicated calculations, a substitution is made to solve the expression easily. The input power P_{in_Tx}, which is the emitted power as shown in Fig. 1, and P_{in_Rx}, the emitted power when the receiver is excited in the reciprocal situation, are positive real values. Therefore, we can substitute the input powers using a positive real constant α, $P_{in\_Tx} = \alpha P_{in\_Rx}$.

The input power at the receiver antenna (P_{in_Rx}) can be expressed as the sum of the power dissipated inside the enclosed volume (P_{loss_Venc}) and the power that passes through the enclosed surface (P_{thr_Senc}). However, they cannot be combined into a single term because the volume loss power and the power that pass through have different integral regions. Therefore, we use the substitution once more to combine the two powers with a positive real constant β, yielding $P_{in\_Rx} = (1+\beta) P_{thr\_Senc}$. Thus, we have

$$P_{in\_Tx} = \frac{\alpha(1+\beta)}{2} Re\left\{ \oint \left(\mathbf{E_{Rx}} \times \mathbf{H^*_{Rx}}\right) \cdot \mathbf{\hat{n}_{enc}}\, dS_{enc} \right\} \tag{2}$$

where $\mathbf{\hat{n}_{enc}}$ is an outward normal vector from the inside of S_{enc}.

Second, the receiving power, P_{rec_Rx}, in the numerator of the PTE expression can be expressed as the open-circuit voltage (V_{oc_Rx}) at the receiving antenna [22]

$$P_{rec\_Rx} = \frac{1}{8}\frac{\left|V_{oc\_Rx}\right|^2}{R_{ant\_Rx}} \tag{3}$$

$$V_{oc\_Rx} = -\frac{1}{I_{Rx}} \int \left(\mathbf{E_{Tx}} \cdot \mathbf{J_{Rx}} - \mathbf{H_{Tx}} \cdot \mathbf{M_{Tx}}\right) dS_{Rx} \tag{4}$$

where I_{Rx} is the magnitude of the current source of the receiver antenna, and R_{ant_Rx} is the input resistance of the receiver antenna. The reciprocity theorem can be applied to (4) to make the problem easier to solve. It is also assumed that the receiver antenna is matched to the load (Z_{l_Rx}) for maximum PTE

$$P_{rec\_Rx} = \frac{1}{8\left|I_{Rx}\right|^2 R_{l\_Rx}} \left| \int \left(\mathbf{E_{Rx}} \cdot \mathbf{J_{Tx}} - \mathbf{H_{Rx}} \cdot \mathbf{M_{Tx}}\right) dS_{Tx} \right|^2 \tag{5}$$

where $\mathbf{E_{Rx}}$ and $\mathbf{H_{Rx}}$ are the propagating fields of the pilot signals emitted by the receiver antenna. Substituting (2) and (5) into (1) yields

$$\eta = \frac{1}{\alpha\,(1+\beta)^2} \frac{\left|\int \left(\mathbf{E_{Rx}} \cdot \mathbf{J_{Tx}} - \mathbf{H_{Rx}} \cdot \mathbf{M_{Tx}}\right) dS_{Tx}\right|^2}{\left|\oint \left(\mathbf{E_{Rx}} \cdot \mathbf{H^*_{Rx}}\right) \cdot \mathbf{\hat{n}_{enc}} + \left(\mathbf{E^*_{Rx}} \times \mathbf{H_{Rx}}\right) \cdot \mathbf{\hat{n}_{enc}}\, dS_{enc}\right|^2}. \tag{6}$$

B. Maximum PTE

Using scalar triple product and equivalent theorem, the optimal solution for (6) can be found [23], [24]

$$\mathbf{J_{Tx\_opt}} = -k\left(\mathbf{\hat{n}_{enc}} \times \mathbf{H^*_{Rx}}\right) \tag{7a}$$

$$\mathbf{M_{Tx\_opt}} = -k\left(\mathbf{\hat{n}_{enc}} \times \mathbf{E^*_{Rx}}\right) \tag{7b}$$

where k is a proportional constant and $\mathbf{\hat{n}_{enc}}$ is a unit vector toward the outside of the enclosed surface as shown in Fig. 1. Considering equivalent theorem on the transmitting surface

$$\mathbf{E^t_{Tx\_opt}} = k\left(\mathbf{E^t_{Rx}}\right)^* \tag{8a}$$

$$\mathbf{H^t_{Tx\_opt}} = -k\left(\mathbf{H^t_{Rx}}\right)^* \tag{8b}$$

where $\mathbf{E}^{\mathbf{t}}_{\mathbf{Tx\_opt}}$ and $\mathbf{H}^{\mathbf{t}}_{\mathbf{Tx\_opt}}$ are the transmitted field by the optimal current sources, which are tangential to the transmitter surface (S_{Tx}). Now, we substitute the optimal solution (7) into (2) and (9) to find the proportional constant, k

$$P_{in\_Tx} = -\frac{1}{4} Re \int \left(\mathbf{E_{Tx}} \cdot \mathbf{J}^*_{\mathbf{Tx}} + \mathbf{H}^*_{\mathbf{Tx}} \cdot \mathbf{M}'_{\mathbf{Tx}} \right) dS_{Tx}. \tag{9}$$

The substitution becomes

$$|k|^2 = \alpha\,(1+\beta)\,\frac{\frac{1}{2} Re \left\{ \oint \left(\mathbf{E}^{\mathbf{t}}_{\mathbf{Rx}} \times \left(\mathbf{H}^{\mathbf{t}}_{\mathbf{Rx}}\right)^* \right) \cdot \hat{\mathbf{n}}_{\mathbf{enc}}\, dS_{enc} \right\}}{\frac{1}{2} Re \left\{ \int \left(\mathbf{E}^{\mathbf{t}}_{\mathbf{Rx}} \times \left(\mathbf{H}^{\mathbf{t}}_{\mathbf{Rx}}\right)^* \right) \cdot \left(-\hat{\mathbf{n}}_{\mathbf{Tx}}\right) dS_{Tx} \right\}}. \tag{10}$$

As a result, the optimal PTE can be written as below

$$\eta_{opt} = \frac{1}{(1+\beta)} \frac{\left| \frac{1}{2} Re \left\{ \int \left(\mathbf{E}^{\mathbf{t}}_{\mathbf{Rx}} \times \left(\mathbf{H}^{\mathbf{t}}_{\mathbf{Rx}}\right)^* \right) \cdot \left(-\hat{\mathbf{n}}_{\mathbf{Tx}}\right) dS_{Tx} \right\} \right|}{\left| \frac{1}{2} Re \left\{ \oint \left(\mathbf{E}^{\mathbf{t}}_{\mathbf{Rx}} \times \left(\mathbf{H}^{\mathbf{t}}_{\mathbf{Rx}}\right)^* \right) \cdot \hat{\mathbf{n}}_{\mathbf{enc}}\, dS_{enc} \right\} \right|} \tag{11a}$$

$$= \frac{P_{thr\_Senc}}{P_{in\_Rx}}. \tag{11b}$$

Referring to (11), it is worth mentioning that the normal components of the fields (i.e., $\mathbf{E}^{\mathbf{n}}_{\mathbf{Rx}}, \mathbf{H}^{\mathbf{n}}_{\mathbf{Rx}}$) have no effects on the calculation of V_{oc_Rx} and P_{rec_Rx} because the transmission currents (i.e., $\mathbf{J_{Tx}}, \mathbf{M_{Tx}}$) are defined as the tangential components, and only powers passing through the surfaces are used.

In the resulting optimal efficiency from (11), the ratio of the power passing through a specific area (S_{Tx}) to the power passing through the enclosed surface (S_{enc}) is implied, assuming a situation in which the pilot fields are emitted from the receiver. The exact maximum PTE value can be obtained by conducting a full-wave simulation if the input power of the receiving antenna is set as 1 W, and the field quantities of the transmission plane (S_{Tx}) are obtained. By calculating the Poynting vector, we can determine the power passing through a certain area, which is equivalent to the maximum PTE. As the supplied power is the sum of the volume loss power and the through power, ratio β can be easily obtained. In the case of a highly lossy material, the optimal efficiency is very low because the volume loss power in V_{enc} (P_{loss_Venc}) is typically much greater than the passing-through power (P_{thr_Senc}), which results in a large value of β.

Note that the surface waves or reflections between different layers are included in (2). Assume the surface wave propagates toward the x-direction, then the imaginary power in the z-direction at the boundary of S_{enc} is ignored while the real power in the x-direction is included in (2). Therefore, the proposed analysis can be extended to general multilayer structures. However, the distance from any Huygens sources should be at least $\lambda/2\pi$ as mentioned earlier, since we only handle the region where the radiating fields are dominant [20], [21].

It is worth mentioning that a certain area where the through power is high becomes important for S_{Tx} to achieve high efficiency, according to (11). This indicates that areas with a low through power should be avoided so that the transmission area can be efficiently used. By applying this approach, we can determine the maximum PTE when the transmitter is in the limited area.

III. Practical Examples

A. Antennas Implanted in Lossy Media

In this section, the proposed theory is applied to practical scenarios. Representative examples for WPT in lossy media are implantable devices, and this topic has been extensively studied [5]–[15]. In the following examples, an air–skin half-space is assumed, as shown in Fig. 2. The operating frequency is set to the ISM band of 2.4 GHz, though the theory proposed in this communication can be applied to arbitrary frequency bands. The implanted antenna is inserted at a depth of d_{Rx} below the surface, and the transmitting plane is placed d_{Tx} above the interface. For the electric properties of the skin layers, the Cole–Cole model can be referred to [25].

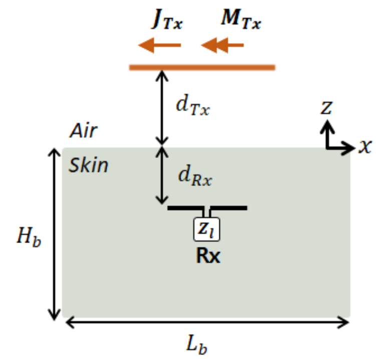

Fig. 2. Configuration for the examples of R-WPT. The ideal transmitting currents (i.e., $\mathbf{J_{Tx}}, \mathbf{M_{Tx}}$) are assumed to flow in the xy plane. The value of d_{Tx} should be properly set, so that it can be a region of R-WPT. A rectangular lossy box is assumed as $L_b = 100$ and $H_b = 60$ (unit: mm).

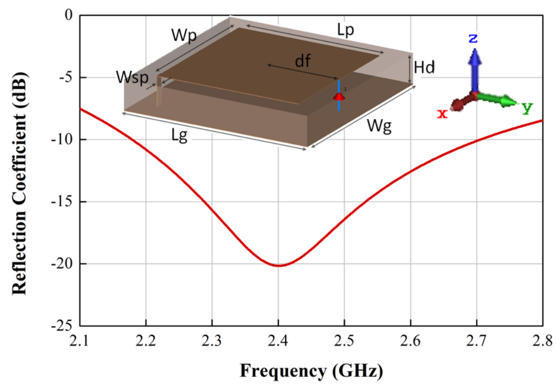

Fig. 3. Configuration of the designed PIFA and its reflection coefficient. The PIFA is embedded in the lossy media as shown in Fig. 2. $L_g = W_g = 5.2$, $L_p = W_p = 4$, $H_d = 0.8$, $d_f = 2$, and $W_{sp} = 0.2$ (unit: mm).

As an example of a receiving antenna for the devices implanted into the skin, a low-profile planar inverted-F antenna (PIFA) is designed, as shown in Fig. 3 [15], [26], [27]. The exact values of each parameter are given in the figure caption. The substrate of the PIFA antenna is Taconic TLC 32, whose ε_r is 3.2 and $\tan\delta$ is 0.009. The receiving antenna is inserted at a depth of 5 mm from the interface, and the transmission surface is placed 120 mm above the interface. As an application of the proposed theory, the maximum PTE of the PIFA antenna, with respect to the size of the transmission area (S_{Tx}), is obtained using CST.

Fig. 4 shows the normalized optimal distributions of the transmission currents. The size of the transmission surface is set as $5\lambda \times 5\lambda$. Fig. 4(a) shows the optimal magnitude of the transmitting electric current density, according to (8). The current vector at the center area is plotted in Fig. 4(b), indicating the optimal polarization of the transmitting antennas. Fig. 4(c) and (d) shows the magnitude and vector of the optimal magnetic current, respectively. Fig. 4(e) shows the square root of the optimal power density. It can integrate the effects of the electric and magnetic currents together. To effectively use the area, the power density below a certain value should be discarded. Fig. 4(f) shows the results without values below 30% of the maximum power density. This indicates that the remaining elliptical area has a significant effect on the PTE. Using this approach, we can determine the bound of the PTE under a certain transmission area.

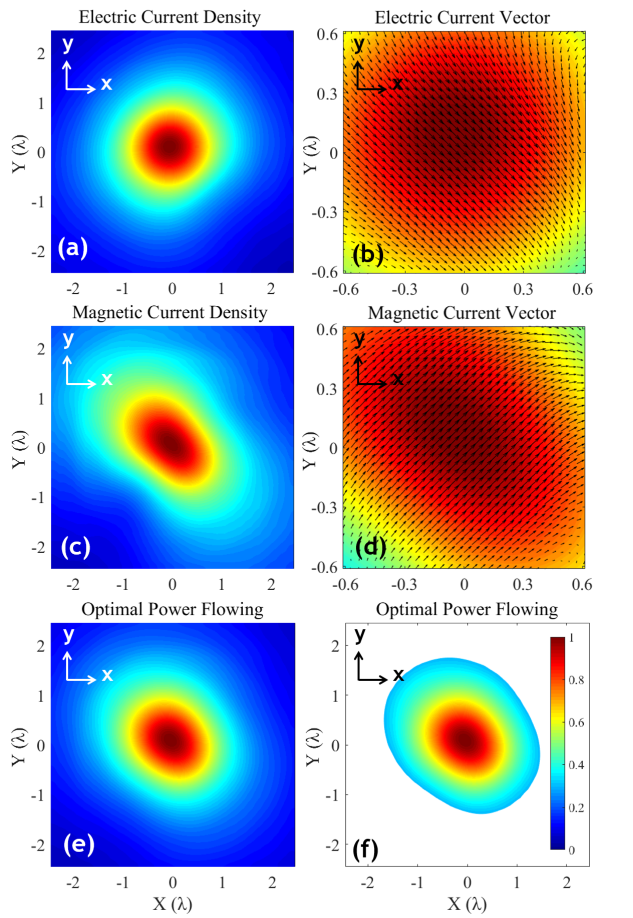

Fig. 4. Normalized distributions of the optimal currents ($\mathbf{J_{Tx}}, \mathbf{M_{Tx}}$) and power density when the PIFA is used as Rx. (a) Magnitude of $\mathbf{J_{Tx}}$. (b) Vector plot by enlarging the center area. (c) Magnitude of $\mathbf{M_{Tx}}$. (d) Vector plot of $\mathbf{M_{Tx}}$. (e) Magnitude of the square root of the optimal power density. (f) Remaining power density after removing the values less than 30% of the maximum power density.

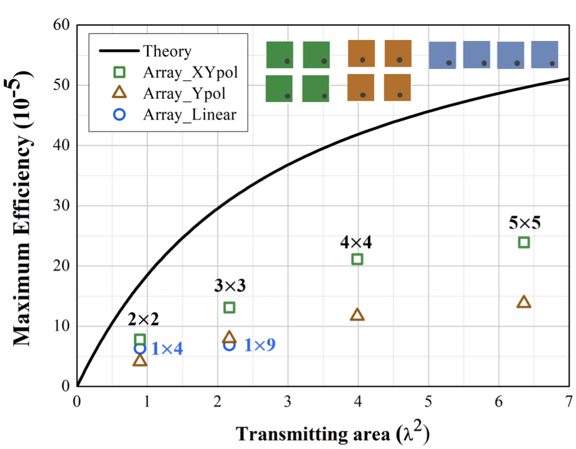

Fig. 5. Maximum efficiency bound for the implanted PIFA. The black line indicates the proposed efficiency bound; the symbols are the results of the actual array antennas with different numbers, polarizations, and arrangements.

Fig. 5 presents the maximum efficiency for the PIFA based on the proposed theory, as indicated by the black solid line. The square symbols in Fig. 5 indicate the maximum efficiency based on the methods proposed in previous studies that calculate the network parameters of the practical rectangular array [14]–[17]. The triangle symbols indicate the results with a cross polarized array, whereas the

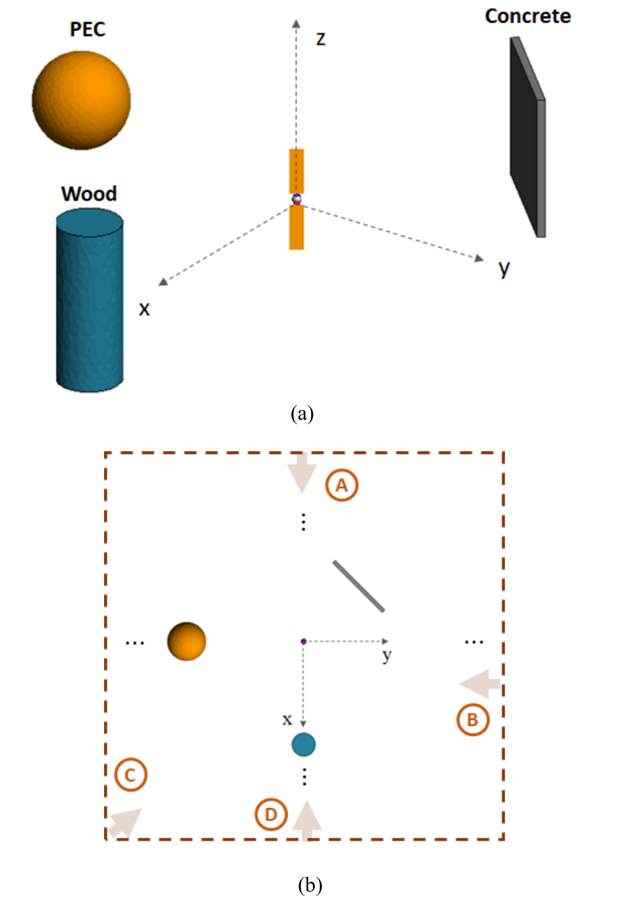

Fig. 6. Configuration of the scattering object scenario. (a) Perspective view of the dipole antenna and three lossy scatterers. (b) Top view of the dipole antenna, scattering objects, and the enclosing virtual transmitting surface. Points A, B, C, and D are indicated on each side.

circles represent the results for a linear array. Considering the total area of the transmission patch array, the maximum PTE is plotted for patch arrays comprising 4, 9, 16, and 25 elements. As shown in Fig. 5, the type and arrangement of the array antenna have a strong influence on the efficient use of the transmission area. The PTE decreases significantly when the polarization is mismatched. The maximum PTE of the linear array is relatively low, as the transmission area is not efficiently used. Therefore, the electric current vector in Fig. 4(b), which can be identified using the proposed theory, should be appropriately considered in the design of the transmitting arrays. The differences between the theoretical bounds and the actual patch arrays are a result of the fact that the rectangular array cannot perfectly reproduce the ideal transmission currents.

It should be noted that the proposed theory could provide fundamental efficiency bounds, which, in turn, would provide a reference guide for the arrangement shape of the transmitting array and polarization of its elements. In addition, the maximum PTE bound could be obtained by conducting a one-time EM simulation when the receiver antenna is in the transmitting mode.

B. Scattered Environments by Lossy Objects

In addition to the implanted case, the theoretical results in (12) could be applied to various scenarios. In particular, when a complex propagation environment is created because of scattering objects near the receivers, the advantages of the proposed theory are clearly presented. Fig. 6 represents a scattering object scenario that makes it difficult to estimate the propagation of EM fields. A half-lambda

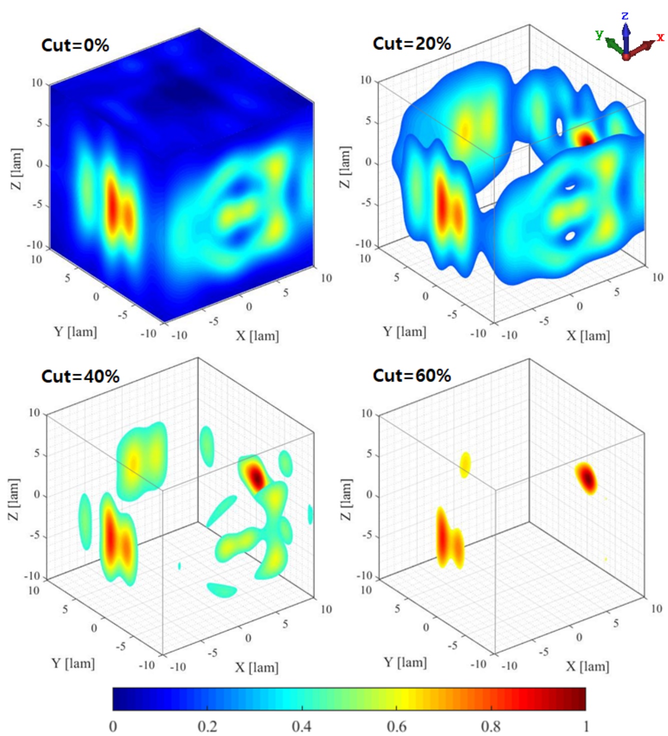

Fig. 7. Normalized distribution of the optimal power density for the receiving dipole antenna with scatterers. The remaining power density after removing the values less than a "cut" value of the maximum value.

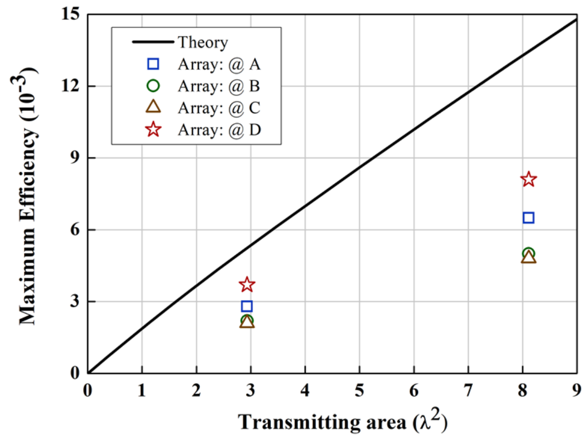

Fig. 8. Maximum efficiency at each location. The black solid line indicates the theoretical bound, whereas the open symbols are the maximum PTE values when the transmitting array is located at each point (one of A, B, C, and D) as shown in Fig. 6. Transmitting rectangular arrays with four and nine elements are used.

TABLE I

MAXIMUM EFFICIENCY VALUES AT DIFFERENT LOCATIONS (UNIT: %)

Array	Theory	@ A	@ B	@ C	@ D
2 × 2 (n=4)	0.52	0.28	0.22	0.21	0.37
3 × 3 (n=9)	1.34	0.65	0.50	0.48	0.81

dipole antenna resonating at 2.4 GHz is located at the origin, and three scatterers are placed around the dipole antenna. A cylindrical rod with a height and radius of 1.5 and 0.3λ, respectively, is placed at a distance of 2.5λ from the z-axis, and a rectangular plate with a length and height of 1.8λ and a thickness of 0.1λ is placed 2λ away from the center at 45°. A conducting sphere with a radius of 0.5λ is placed 3λ away in the y-direction. The cylindrical rod material is set as wood, the rectangular plate is set as concrete, and the material properties are imported from the library available in FEKO.

In the example presented in Section III-A, the location of the transmitter could be determined easily. However, in a situation where the field distribution is complicated by the presence of scattering objects, the selection of the transmitter location becomes an important issue. Fig. 6(b) presents the top view of the scattered scenario used in this example with a virtual 3-D transmitting surface of 20λ × 20λ × 20λ.

Since there is no comment on deciding the optimal placement of the transmitting array in the previous studies, the transmitter can be placed at arbitrary spots and iteratively measured to find its best placement. Here, three intuitive locations on the transmitting surface are marked as A, B, and C. Location A is at the center of the yz-plane, B is located 2λ away from the center of the xz-plane, and C is set facing the rectangular concrete wall. However, measuring the network parameters at expected positions requires a considerable amount of time and effort. Moreover, there is no guarantee that the optimum position and polarization will be found.

On the other hand, when the proposed theory is used, it is possible to derive the optimal transmitting current (or power density), which can then be used to determine the optimal location for the transmitting arrays when lossy scatterers exist. The normalized optimal power density distribution on the transmitting surface is shown in Fig. 7. The optimal power density values are removed from the lowest values, resulting in the preferential spots where the transmitter should be placed. As can be observed in Fig. 7, the optimal current is strong on the yz-plane. In particular, the optimal current is strongest on the plane located at the rear of the cylindrical rod, indicated as location D in Fig. 6(b), which is a different location from that of the general intuition. Furthermore, the optimal current distribution is not concentrated on one plane but is distributed along other planes. Therefore, to maximize the PTE when lossy scattering exists, distributed transmitters would be advantageous.

Fig. 8 describes the simulated maximum PTE values when two types of transmitting arrays (i.e., 2 × 2 and 3 × 3) are placed at each location (A, B, C, and D) shown in Fig. 6. The black solid line indicates the theoretical maximum efficiency bound, whereas the open rectangular, circular, triangular, and star symbols indicate the PTE when the transmitting array is placed at A, B, C, and D, respectively. The star symbols represent the PTE referring the optimal power density derived by the proposed theory. The maximum PTEs are calculated using network parameters [14]–[17], and the maximum PTEs at each location are presented in Table I. The PTE at the optimal position (i.e., D) increased 32% relative to that at A and 76% relative to that at C for the 2 × 2 array. For the 3 × 3 array, the PTE increased from as little as 25% to as much as 69% relative to A and C, respectively. These results clearly demonstrate that the maximum PTE can increase when the location of the transmitting array is properly determined. It is worth noting that even if the transmitting array is placed in the optimal location, a discrepancy with the theoretical bound could arise because the actual array cannot operate as ideal currents.

IV. CONCLUSION

In this study, we present a theoretical analysis of the optimal transmission currents for receivers when lossy materials exist. The results show that a tangential part of the fields radiated by the receiver must be considered to maximize the PTE with lossy media.

Using the analysis, we determined the maximum bound of the PTE when the available transmission area is limited as well as the optimal placement of the transmitting array. Two examples are presented to demonstrate the usability of the proposed theory and to compare it with previous works. Through these examples, we showed that the radiation characteristics of the receiver antenna play a significant role in determining the PTE, especially in lossy environments. We believe that this communication can be useful in the development of R-WPT systems for an increased number of practical applications with lossy media.

References

[1] G. Goubau and P. Schwering, "Free space beam transmission," in *Microwave Power Engineering*, vol. 1, C. Okress, Ed. New York, NY, USA: Academic, 1968, pp. 241–255.

[2] W. Brown, "Experiments involving a microwave beam to power and position a helicopter," *IEEE Trans. Aerosp. Electron. Syst.*, vol. AES-5, no. 5, pp. 692–702, Sep. 1969.

[3] N. Shinohara, "Power without wires," *IEEE Microw. Mag.*, vol. 12, no. 7, pp. S64–S73, Dec. 2011.

[4] J.-H. Kim, Y. Lim, and S. Nam, "Efficiency bound of radiative wireless power transmission using practical antennas," *IEEE Trans. Antennas Propag.*, vol. 67, no. 8, pp. 5750–5755, Aug. 2019.

[5] C. T. Tai and R. E. Collin, "Radiation of a Hertzian dipole immersed in a dissipative medium," *IEEE Trans. Antennas Propag.*, vol. 48, no. 10, pp. 1501–1506, Oct. 2000.

[6] M. S. Mirmoosa, S. Nordebo, and S. A. Tretyakov, "Physical meaning of the dipole radiation resistance in lossless and lossy media: What is the radiation resistance of antennas in lossy media?" *IEEE Antennas Propag. Mag.*, vol. 62, no. 4, pp. 75–81, Aug. 2020.

[7] K. M. Z. Shams and M. Ali, "Wireless power transmission to a buried sensor in concrete," *IEEE Sensors J.*, vol. 7, no. 12, pp. 1573–1577, Dec. 2007.

[8] S. Jiang and S. V. Georgakopoulos, "Optimum wireless powering of sensors embedded in concrete," *IEEE Trans. Antennas Propag.*, vol. 60, no. 2, pp. 1106–1113, Feb. 2012.

[9] A. S. Y. Poon, S. O'Driscoll, and T. H. Meng, "Optimal frequency for wireless power transmission into dispersive tissue," *IEEE Trans. Antennas Propag.*, vol. 58, no. 5, pp. 1739–1750, May 2010.

[10] S. Kim, J. S. Ho, and A. S. Y. Poon, "Wireless power transfer to miniature implants: Transmitter optimization," *IEEE Trans. Antennas Propag.*, vol. 60, no. 10, pp. 4838–4845, Oct. 2012.

[11] R. Das and H. Yoo, "A multiband antenna associating wireless monitoring and nonleaky wireless power transfer system for biomedical implants," *IEEE Trans. Microw. Theory Techn.*, vol. 65, no. 7, pp. 2485–2495, Jul. 2017.

[12] K. Zhang *et al.*, "Near-field wireless power transfer to deep-tissue implants for biomedical applications," *IEEE Trans. Antennas Propag.*, vol. 68, no. 2, pp. 1098–1106, Feb. 2020.

[13] Z. Nie and Y. Yang, "A model independent scheme of adaptive focusing for wireless powering to in-body shifting medical device," *IEEE Trans. Antennas Propag.*, vol. 66, no. 3, pp. 1497–1506, Mar. 2018.

[14] Z. Duan, L.-J. Xu, S. Gao, and G. Wen, "Integrated design of wide-band omnidirectional antenna and electronic components for wireless capsule endoscopy systems," *IEEE Access*, vol. 6, pp. 29626–29636, 2018.

[15] Z. Chen, H. Sun, and W. Geyi, "Maximum wireless power transfer to the implantable device in the radiative near field," *IEEE Antennas Wireless Propag. Lett.*, vol. 16, pp. 1780–1783, 2017.

[16] W. Geyi, *Foundations of Applied Electrodynamics*. Hoboken, NJ, USA: Wiley, 2010.

[17] L. Shan and W. Geyi, "Optimal design of focused antenna arrays," *IEEE Trans. Antennas Propag.*, vol. 62, no. 11, pp. 5565–5571, Nov. 2014.

[18] H.-T. Chou, "Conformal near-field focus radiation from phased array of antennas to enhance power transfer between transmitting and receiving antennas," *IEEE Trans. Antennas Propag.*, vol. 68, no. 5, pp. 3567–3577, May 2020.

[19] H.-T. Chou, "Maximization of mutual reaction between two conformal phased arrays of antennas to enhance power transfer in radiating near-field region," *IEEE J. Radio Freq. Identificat.*, vol. 4, no. 4, pp. 506–516, Dec. 2020.

[20] C. A. Balanis, *Antenna Theory: Analysis and Design*, 3rd ed. Hoboken, NJ, USA: Wiley, 2005.

[21] W. L. Stutzman and G. A. Thiele, *Antenna Theory and Design*, 2nd ed. New York, NY, USA: Wiley, 1998.

[22] R. G. Harrington, *Time-Harmonic Electromagnetic Fields*. Piscataway, NJ, USA: IEEE Press, 2001.

[23] G. Strang, *Linear Algebra and its Applications*, 4th ed. Toronto, ON, Toronto, Thomson, 2006.

[24] G. H. Golub and C. F. Van Loan, *Matrix Computations*, 4th ed. Baltimore, MD, USA: Johns Hopkins Univ. Press, 2013.

[25] S. Gabriel, R. W. Lau, and C. Gabriel, "The dielectric properties of biological tissues: III. Parametric models for the dielectric spectrum of tissues," *Phys. Med. Biol.*, vol. 41, no. 11, p. 2271, 1996.

[26] C. Liu, Y.-X. Guo, H. Sun, and S. Xiao, "Design and safety considerations of an implantable rectenna for far-field wireless power transfer," *IEEE Trans. Antennas Propag.*, vol. 62, no. 11, pp. 5798–5806, Nov. 2014.

[27] M. C. Huynh and W. Stutzman, "Ground plane effects on planar inverted-F antenna (PIFA) performance," *IEE Proc.-Microw., Antennas Propag.*, vol. 150, no. 4, pp. 209–213, 2003.